Research Article | Vol. 25, No. 7 | 3 Apr 2017 | OPTICS EXPRESS 8450

Optics EXPRESS

Dissection of electron correlation in strong-field sequential double ionization using a classical model

YUEMING ZHOU,[1] MIN LI,[1,*] YANG LI,[1] AIHONG TONG,[2] QIANGUANG LI,[3] AND PEIXIANG LU[1,4,5]

[1]*Wuhan National Laboratory for Optoelectronics and School of Physics, Huazhong University of Science and Technology, Wuhan 430074, China*
[2]*Department of Physics and Mechanical and Electrical Engineering, Hubei University of Education, Wuhan 430205, China*
[3]*School of Physics and Electronic-information Engineering, Hubei Engineering University, Xiaogan 432000, China*
[4]*Laboratory of Optical Information Technology, Wuhan Institute of Technology, Wuhan 430205, China*
[5]*lupeixiang@mail.hust.edu.cn*
[*]*mli@hust.edu.cn*

Abstract: Recent experiments on strong-field sequential double ionization (SDI) have reported several observations which are regarded as evidence of electron correlation, querying the validity of the standard independent electron approximation for SDI. Here we theoretically study SDI with a classical ensemble model. The experimental results are well reproduced with this model. Back tracing of the ionization process shows that these results are ascribed to the subcycle ionization dynamics of the two electrons, not the evidences of the electron correlation in SDI. Thus, the previously reported observations are not enough to claim the breakdown of the independent electron approximation in SDI.

OCIS codes: (020.4180) Multiphoton processes; (270.6620) Strong-field processes; (260.3230) Ionization.

References and links

1. F. Krausz and M. Ivanov, "Attosecond physics," Rev. Mod. Phys. **81**(1), 163–234 (2009).
2. M. He, Y. Li, Y. Zhou, M. Li, and P. Lu, "Temporal and spatial manipulation of the recolliding wave packet in strong-field photoelectron holography," Phys. Rev. A **93**(3), 033406 (2016).
3. C. Zhai, L. He, P. Lan, X. Zhu, Y. Li, F. Wang, W. Shi, Q. Zhang, and P. Lu, "Coulomb-corrected molecular orbital tomography of nitrogen," Sci. Rep. **6**, 23236 (2016).
4. L. Li, Z. Wang, F. Li, and H. Long, "Efficient generation of highly elliptically polarized attosecond pulses," Opt. Quantum Electron. **49**, 73 (2017).
5. X. Zhang, X. Zhu, X. Liu, D. Wang, Q. Zhang, P. Lan, and P. Lu, "Ellipticity-tunable attosecond XUV pulse generation with a rotating bichromatic circularly polarized laser field," Opt. Lett. **42**, 1027–1030 (2017).
6. Z. Wang, M. Li, Y. Zhou, P. Lan, and P. Lu, "Correlated electron-nuclear dynamics in above-threshold multiphoton ionization of asymmetric molecule," Sci. Rep. **7**, 42585 (2017).
7. M. Qin and X. Zhu, "Molecular orbital imaging for partially aligned molecules," Opt. Laser Technol. **87**, 79–86 (2017).
8. C. Zhai, X. Zhu, P. Lan, F. Wang, L. He, W. Shi, Y. Li, M. Li, Q. Zhang, and P. Lu, "Diffractive molecular-orbital tomography," Phys. Rev. A **95**(3), 033420 (2017).
9. A. l'Huillier, L. A. Lompre, G. Mainfray, and C. Manus, "Multiply charged ions induced by multiphoton absorption in rare gases at 0.53 μm," Phys. Rev. A **27**(5), 2503–2512 (1983).
10. B. Walker, B. Sheehy, L. F. Dimauro, P. Agostini, K. J. Schafer, and K. C. Kulander, "Precision measurement of strong field double ionizaiton of helium," Phys. Rev. Lett. **73**(9), 1227–1230 (1994).
11. M. Weckenbrock, D. Zeidler, A. Staudte, Th. Weber, M. Schöfler, M. Meckel, S. Kammer, M. Smolarski, O. Jagutzki, V. Bhardwaj, D. Rayner, D. Villeneuve, P. Corkum, and R. Döner, "Fully differential rates for femtosecond multiphoton double ionization of neon," Phys. Rev. Lett. **92**(21), 213002 (2004).
12. A. Rudenko, K. Zrost, B. Feuerstein, V. L. B. de Jesus, C. D. Schröer, R. Moshammer, and J. Ullrich, "Correlated multielectron dynamics in ultrafast laser pulse interactions with atoms," Phys. Rev. Lett. **93**(25), 253001 (2004).
13. P. B. Corkum, "Plasma perspective on strong-field multiphoton ionization," Phys. Rev. Lett. **71**(13), 1994–1997 (1993).

#287491 https://doi.org/10.1364/OE.25.008450
Journal © 2017 Received 24 Feb 2017; revised 22 Mar 2017; accepted 23 Mar 2017; published 31 Mar 2017

Optics EXPRESS

14. Th. Weber, H. Giessen, M. Weckenbrock, G. Urbasch, A. Staudte, L. Spielberger, O. Jagutzki, V. Mergel, M. Vollmer, and R. Döner, "Correlated electron emmision in multiphoton double ionization," Nature(London) **405**, 658–661 (2000).
15. Y. Zhou, P. Lu, "Correlated electron dynamics in strong-field double ionization (in Chinese)," Sci. Sin-Phys. Mech. Astron. **47**, 033005 (2017).
16. A. Becker, R. Döner, and R. Moshammer, "Multiple fragmentation of atoms in femtosecond laser pulses," J. phys. B **38**(9), S753–s772 (2005).
17. W. Becker, X. Liu, Phay J. Ho, and J. Eberly, "Theories of photoelectron correlation in laser-driven multiple atomic ionization," Rev. Mod. Phys. **84**(3), 1011–1043 (2012).
18. A. Staudte, C. Ruiz, M. Schöfler, S. Schösler, D. Zeidler, Th. Weber, M. Meckel, D. Villeneuve, P. Corkum, A. Becker, and R. Döner, "Binary and recoil collisions in strong field double ionization of helium," Phys. Rev. Lett. **99**(26), 263002 (2007).
19. B. Bergues, M. Küel, N. Johnson, B. Fischer, N. Camus, K. Betsch, O. Herrwerth, A. Senftleben, A. Sayler, T. Rathje, T. Pfeifer, I. Ben-Itzhak, R. Jones, G. Paulus, F. Krausz, R. Moshammer, J. Ullrich, and M. Kling, "Attosecond tracing of correlated electron-emission in non-sequential double ionization," Nat. Commun. **3**, 813 (2012).
20. X. Sun, M. Li, D. Ye, G. Xin, L. Fu, X. Xie, Y. Deng, C. Wu, J. Liu, Q. Gong, and Y. Liu, "Mechanisms of Strong-Field Double Ionization of Xe," Phys. Rev. Lett. **113**(10), 103001 (2014).
21. L. Zhang, X. Xie, S. Roither, Y. Zhou, P. Lu, D. Kartashov, M. Schöfler, D. Shafir, P. Corkum, A. Baltuša, A. Staudte, and M. Kitzler, "Subcycle Control of Electron-Electron Correlation in Double Ionization," Phys. Rev. Lett. **112**(19), 193002 (2014).
22. S. Haan, L. Breen, A. Karim, and J. H. Eberly, "Variable time lag and backward ejection in full-dimension analysis of strong field double ionization," Phys. Rev. Lett. **97**(10), 103008 (2006).
23. D. Ye, M. Li, L. Fu, J. Liu, Q. Gong, Y. Liu, and J. Ullrich, "Scaling Laws of the Two-Electron Sum-Energy Spectrum in Strong-Field Double Ionization," Phys. Rev. Lett. **115**(12), 123001 (2015).
24. X. Ma, Y. Zhou, and P. Lu, "Multiple recollisions in strong-field nonsequential double ionization," Phys. Rev. A **93**(1), 013425 (2016).
25. C. Huang, W. Guo, Y. Zhou, and Z. Wu, "Role of Coulomb repulsion in correlated-electron emission from a doubly excited state in nonsequential double ionization of molecules," Phys. Rev. A **93**(1), 013425 (2016).
26. C. Maharjan, A. Alnaser, X. Tong, B. Ulrich, P. Ranitovic, S. Ghimire, Z. Chang, I. Litvinyuk, and C. Cocke, "Momentum imaging of doubly charged ions of Ne and Ar in the sequential ionization region," Phys. Rev. A **72**(4), 041403R (2005).
27. A. Pfeiffer, C. Cirelli, M. Smolarski, R. Döner, and U. Keller, "Timing the release in sequential double ionization," Nat. Phys. **7**, 428–433 (2011).
28. P. Wustelt, M. Möler, T. Rathje, A. M. Sayler, T. Stölker, and G. G. Paulus, "Momentum-resolved study of the saturation intensity in multiple ionization," Phys. Rev. A **91**(3), 031401R (2015).
29. X. Wang and J. H. Eberly, "Effects of elliptical polarization on strong-field short-pulse double ionization," Phys. Rev. Lett. **103**(10), 103007 (2009).
30. A. Fleischer, H. Wöner, L. Arissian, L. Liu, M. Meckel, A. Rippert, R. Döner, D. M. Villeneuve, P. Corkum, and A. Staudte, "Probing Angular Correlations in Sequential Double Ionization," Phys. Rev. Lett. **107**(11), 113003 (2011).
31. L. Fechner, N. Camus, J. Ullrich, T. Pfeifer, and R. Moshammer, "Strong-Field Tunneling from a Coherent Superposition of Electronic States," Phys. Rev. Lett. **112**(21), 213001 (2014).
32. A. Pfeiffer, C. Cirelli, M. Smolarski, X. Wang, J. Eberly, R. Döner, and U. Keller, "Breakdown of the independent electron approximation in sequential double ionization," New J. Phys. **13**, 093008 (2011).
33. X. Wang and J. Eberly, "Multielectron Effects in Sequential Double Ionization with Elliptical Polarization," arXiv:1102.0221v1.
34. Y. Zhou, C. Huang, Q. Liao, and P. Lu, "Classical Simulations Including Electron Correlations for Sequential Double Ionization," Phys. Rev. Lett. **109**(5), 053004 (2012).
35. J. Parker, B. Doherty, K. Taylor, K. Schultz, C. Blaga, and L. DiMauro, "High-Energy Cutoff in the Spectrum of Strong-Field Nonsequential Double Ionization," Phys. Rev. Lett. **96**(13), 133001 (2006).
36. S. Hu, "Boosting Photoabsorption by Attosecond Control of Electron Correlation," Phys. Rev. Lett. **111**(12), 123003 (2013).
37. A. Liu and U. Thumm, "Laser-assisted XUV few-photon double ionization of helium: Joint angular distributions," Phys. Rev. A **89**(6), 063423 (2014).
38. Y. Zhou, C. Huang, A. Tong, Q. Liao, and P. Lu, "Correlated electron dynamics in nonsequential double ionization by orthogonal two-color laser pulses," Opt. Express **19**(3), 2301–2308 (2011).
39. A. Tong, Y. Zhou, and P. Lu, "Resolving subcycle electron emission in strong-field sequential double ionization," Opt. Express **23**(12), 15774–15783 (2015).
40. A. Tong, Y. Zhou, and P. Lu, "Bifurcation of ion momentum distributions in sequential double ionization by elliptically polarized laser pulses," Opt. Quantum Electron. **49**, 77 (2017).
41. M. Schöfler, X. Xie, P. Wustelt, M. Möler, S. Roither, D. Kartashov, A. Sayler, A. Baltuska, G. Paulus, and M. Kitzler, "Laser-subcycle control of sequential double-ionization dynamics of helium," Phys. Rev. A **93**(6), 063421 (2016).
42. P. Wang, A. Sayler, K. Carnes, B. Esry, and I. Ben-Itzhak, "Disentangling the volume effect through intensity-

Optics EXPRESS

difference spectra: application to laser-induced dissociation of H_2^+," Opt. Lett. **30**(6), 664-666 (2005).
43. P. Wustelt, M. Möller, Markus S. Schöffler, X. Xie, V. Hanus, A. Max Sayler, A. Baltuska, Gerhard G. Paulus, and M. Kitzler, "Numerical investigation of the sequential-double-ionization dynamics of helium in different few-cycle-laser-field shapes," Phys. Rev. A **95**(2), 023411 (2017).

1. Introduction

Strong-field double ionization is a fundamental process in intense laser-matter interaction [1–8] and has attracted intensive attention during the past decades [9–12]. Generally, strong-field double ionization occurs through two different pathways, sequential double ionization (SDI) and nonsequential double ionization (NSDI). In NSDI, the first tunneling ionized electron returns back to the parent ion when the electric field of the laser changes its direction, and kicks out the second electron through an inelastic recollision [13]. Because of this recollision, the electron pairs reveal a highly correlated behavior [14, 15]. The particular interest in strong-field double ionization is the dynamics of this type of electron correlation. Nowadays, the microscopic dynamics of the correlated electrons in NSDI has been profoundly understood with the state-of-art experimental techniques and theoretical methods [16–25]. In the elliptically polarized laser pulses, recollision is strongly suppressed and thus double ionization is dominated by SDI where the two electrons are ionized one after the other by the laser field. Recently, SDI by the elliptical laser pulses has also attracted much attention because it could provide much information about the tunneling ionization of two electrons [26–29]. In SDI it was widely accepted that electron correlation had no effect on the ionization of the two electrons and they could be treated independently. However, this independent electron approximation has been questioned by recent experiments. For example, in a pump-probe experiment, a clear angular correlation between the two electrons in SDI was observed [30]. While this correlation has been interpreted as the dynamics of the hole left by the ionization of the first electron [30, 31], two other phenomena reported in the attoclock experiment are much more confusing [32]. In that experiment, it was observed that the ratio of the parallel and antiparallel emissions of the two electrons in SDI by the elliptical laser pulses shows an oscillating behavior as a function of the laser intensity. This is in contrast with the independent electron approximation which predicts a ratio of unity, independent of the laser intensity. We mention that this oscillating behavior has been observed in recent numerical studies with classical ensemble models but no explanation was proposed [33, 34]. Another observation is the shapes of the differential momentum spectrum of the two electrons in the direction of the minor polarization axis of the laser field. The experimental results show that the distributions exhibit different shapes for the parallel and antiparallel emission events [32], in contrast to the prediction of the independent electron approximation which predicts the same shape for the parallel and antiparallel events. These two results, though very faint, shocked people's understanding on SDI. It was speculated that the independent electron approximation for SDI might break down and the electron correlation should be taken into account [32]. However, this speculation has not been confirmed. Are the above phenomena really the effects of electron correlation, and to what extent the SDI dynamics is affected by electron correlation?

In this paper, we theoretically studied SDI by elliptical laser pulses with a classical ensemble model. The experimental results were well reproduced by this classical model. We explored the responsible dynamics for these results by back tracing the classical trajectories. It was shown that both results, which have been regarded as the effects of electron correlation, are ascribed to the subcycle nature of the ionization dynamics in SDI by elliptical laser pulses. Neglecting the electron correlation could well explain the experimental results and thus they are not strong enough to claim the breakdown of the independent electron approximation in SDI.

Optics EXPRESS

2. Numerical method

The difficulty in identifying the physical origin of the subtle effects in SDI is the lacking of accurate theoretical model. The most accurate model for SDI is numerically solving the two-electron time-dependent Schrödinger equation [35–37]. However, its numerical demand is extremely huge and at present it has only been applied to double ionization by the linearly polarized laser pulses. Extending it to the elliptical laser pulses seems impossible in the near feature. Instead, classical methods have been widely used to study the double and multiple ionizations in strong laser fields [22–24]. It has been demonstrated that the classical models are very successful not only in explaining the experimental data [22,23] but also in predicting new phenomena [21,38]. Recently, we have developed a classical ensemble model which is very accurate and efficient in studying SDI [34]. For example, the experimentally measured ionization times of the two electrons in SDI by the elliptical laser pulses, for which the standard tunneling model failed, were well reproduced by our classical model [34]. With this model, we also predicted the multiple ionization bursts in SDI by the elliptical pulses [39,40] and it was experimentally observed soon [41]. Here, we employ this classical ensemble model to dissect the experimentally observed features of electron correlation in SDI. In this model, the double ionization process is governed by the classical equation of motion [34] (atomic units are used throughout unless stated otherwise),

$$\frac{d\mathbf{r}_i}{dt} = \frac{\partial \mathrm{H}}{\partial \mathbf{p}_i}, \frac{d\mathbf{p}_i}{dt} = -\frac{\partial \mathrm{H}}{\partial \mathbf{r}_i}, \tag{1}$$

where

$$\mathrm{H} = \frac{1}{|\mathbf{r}_1 - \mathbf{r}_2|} + \sum_{\mathrm{i}=1,2} [-\frac{2}{\mathrm{r_i}} + \frac{\mathbf{p}_\mathrm{i}^2}{2} + \mathrm{V_H}(\mathrm{r_i}, \mathrm{p_i})] + [\mathbf{r}_1 + \mathbf{r}_2] \bullet \mathbf{E}(\mathrm{t}) \tag{2}$$

is the Hamiltonian of the two-electron system in the presence of the laser field $\mathbf{E}(t)$. $\mathbf{r}_i$ and $\mathbf{p}_i$ are the position and canonical momentum of the ith electron, respectively. The electric field is written as

$$\mathbf{E}(t) = f(t)[\frac{1}{\sqrt{\varepsilon^2+1}}\cos(\omega t + \varphi)\hat{\mathbf{x}} + \frac{\varepsilon}{\sqrt{\varepsilon^2+1}}\sin(\omega t + \varphi)\hat{\mathbf{y}}], \tag{3}$$

where ω, ε and φ are the laser frequency, the ellipticity and carrier-envelope phase (CEP), respectively. $f(t)$=$E_0\cos(\frac{\pi t}{NT_0})^2$ is the field envelope (T_0 is the laser period and N indicates number of laser cycles). $V_H(r_i, p_i)$ is the Heisenberg-core potential, which is expressed as [34],

$$V_H(r_i, p_i) = \frac{\xi^2}{4\alpha r_i^2} exp\{\alpha[1 - (\frac{r_i p_i}{\xi})^4]\}. \tag{4}$$

The parameter α indicates the rigidity of the Heisenberg core and is chosen to be 2 in this paper. For a given α, the parameter ξ is chosen to match the second ionization potential of the target. Here we set ξ=1.225 for target Ar [34].

To obtain the initial state, the two electrons were firstly placed at the classical allowed region and the available kinetic energy was distributed between the two electrons randomly in phase space. Then the system was evolved at the absence of the laser field for a sufficiently long time to obtain a stable distribution in the phase space [34]. After the initial state was obtained, the evolution of the system was governed by Eq. (1). When the laser field was turned off, we collected the double ionization events, where double ionization is defined if the final energies of both electrons are positive. In our calculations, the ellipticity of laser pulses is $\varepsilon = 0.75$ so that recollision is strongly suppressed and all of the double ionizations are SDI.

3. Results and discussions

We first show the momentum distributions of the doubly charged ion in Fig.1. Figure 1(a) displays the ion momentum distribution in the laser polarized plane, where the laser intensity is 1.5

Optics EXPRESS

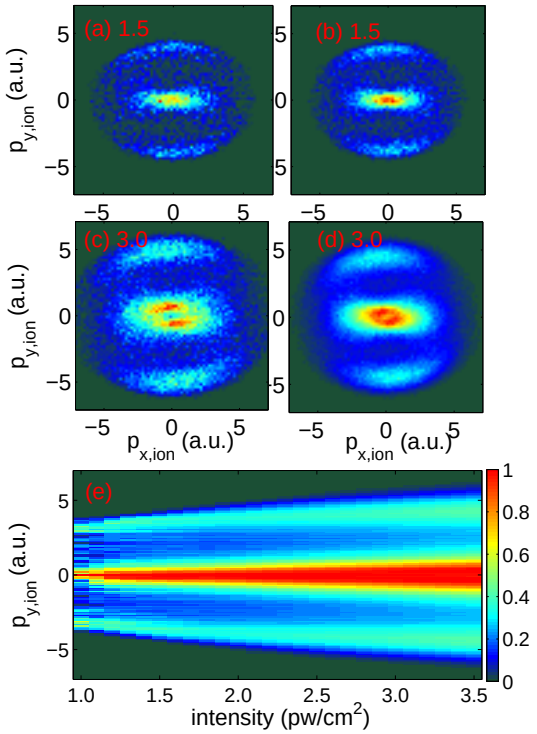

Fig. 1. (a) Momentum distribution of the doubly charged ion in the laser polarization plane. The laser intensity, ellipticity, and pulse duration are 1.5 PW/cm^2, ε = 0.75, and N=6, respectively. The CEP is randomly chosen for each trajectory. (b) The same as (a) but with the laser focal volume assuming a Gaussian beam profile taken into accounts. (c) (d) The same as (a) and (b), respectively, but with the laser intensity of 3.0 PW/cm^2. (e) Momentum distribution of the ion along the minor axis of the laser polarization plane as a function of the laser intensity, where the laser focal volume effect has been considered. The ensemble sizes are chosen so that more than 10^4 SDI events are collected at each laser intensity.

PW/cm^2 and the pulse duration N=6. The CEP is randomly set for each atom in the ensemble. Technically, the CEP for each atom in the ensemble was generated by a random number between 0 and 2π. This corresponds to a CEP-unlocked experiment. In Fig. 1(b) the laser parameters are the same as Fig. 1(a) but with the laser focal volume effect taken into account [42]. It was seen that the distributions exhibit a three-peak structure along the minor axis of the laser polarization plane. Figure 1(c) shows the distribution for a higher intensity of 3.0 PW/cm^2. The distribution exhibits a four-peak structure at this laser intensity. When the laser focal volume effect is considered, the inner two peaks are almost unresolvable and the spectrum shows a three-peak structure, as shown in Fig. 1(d). The three-peak and four-peak structures are consistent with the previous experimental data [27, 32] and have been well understood. The outer and inner peaks correspond to the two electrons emitted into the same and opposite hemispheres, respectively [27]. At low laser intensities, both electrons ionized around the peak of the laser pulses and thus the magnitude of the two electrons' final momentum are almost the same. Therefore, the ion for the antiparallel emission SDI achieved nearly zero final momentum, resulting in the three-peak structure [34]. Figure 1(e) shows the evolution of this peak structure as a function of laser intensity. The spectrum always exhibits a three-peak structure when the laser focal volume effect was taken into account.

Optics EXPRESS

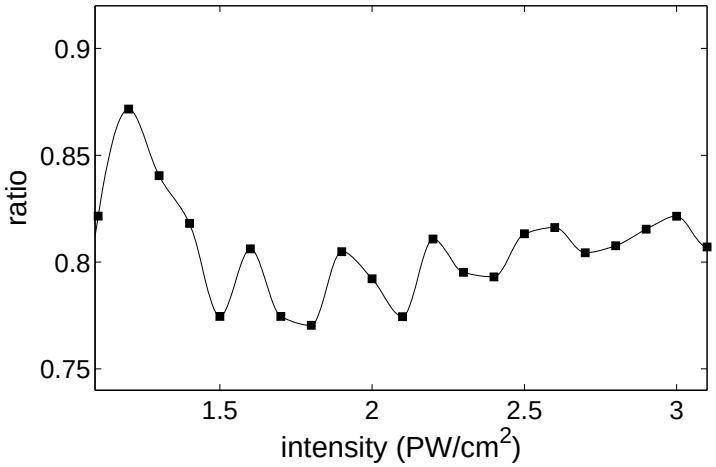

Fig. 2. The ratio of the parallel and antiparallel emission SDI events as a function of the laser intensity. The pulse parameters are the same as those in Fig. 1. The CEP are randomly chosen for each trajectory in the ensemble.

To gain deeper insights into the SDI process, in Fig. 2 we show the ratio of the parallel and antiparallel SDI events as a function of the laser intensity. In the previous experiment, it was shown that the ratio oscillated with laser intensity [32]. The oscillating behavior from our calculations in Fig. 2 is also obvious. We mention that this oscillating behavior does not result from the statistic uncertainty of our calculations, which has been confirmed by enlarging the ensemble size. It was expected that the emission direction of the second electron did not depend on the emission direction of the first electron if there was no correlation between the two electrons. Thus the ratio of parallel and antiparallel emission should be unity and independent of the laser intensity within the independent electron approximation [32]. The observed oscillation naturally leads to the speculation of the breakdown of the independent electron approximation in SDI [32]. As we will show below, this speculation is questionable.

The parallel and antiparallel emissions in SDI depend on the time delay between the ionization of the two electrons. In Fig. 3 we show the ionization time distributions of the two electrons. Here, the ionization time is defined as the instant when the electron achieves positive energy and it is obtained by back tracing the SDI trajectories. In the elliptical laser pulses, the ionization picture of SDI is that there is a subcycle ionization burst during each half cycle when the transient laser electric field vector points along the major axis of the laser polarization plane. Thus, during the laser pulses there are several subcycle ionization bursts for each electron, as shown in Figs. 3(a)-3(c). We mention that these subcycle ionization bursts have been observed very recently [41]. In Figs. 3(d)-3(f) we show the ionization time distributions of the first electron versus the second electron. A time delay of even half cycles results in the parallel emissions. The population indicated by the red solid boxes corresponds to this type of emissions. The population indicated by the gray dashed boxes corresponds to the time delay of odd half cycles and leads to the antiparallel emission SDI events. It is easy to expect that the subcycle ionization bursts of the two electrons vary with laser intensity [comparing Figs. 3(a)-3(c)], and thus the distribution of the time delay changes with laser intensity, as shown in Fig. 4. This explains the oscillating behavior in Fig.2.

The analysis above indicates that the oscillation can be understood as the subcycle nature of

Optics EXPRESS

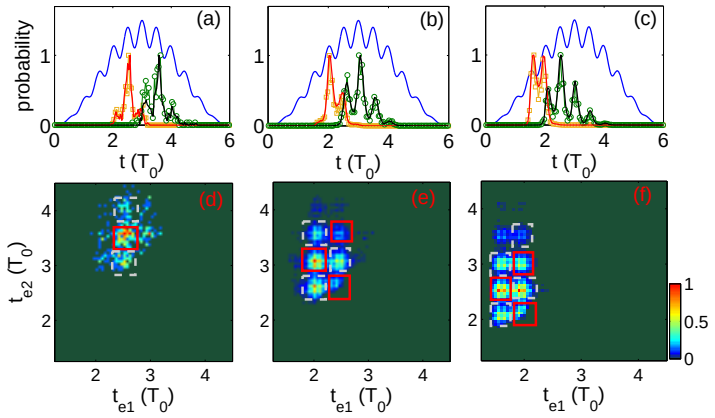

Fig. 3. (a)-(c) Ionization time distributions for the first (the red lines) and the second electrons (the black lines). The laser intensities in (a)-(c) are 1.0 PW/cm^2, 2.0 PW/cm^2, and 3.5 PW/cm^2, respectively. The blue lines indicate the magnitude of the electric field of the laser pulses. The yellow squares and the green circles present the ionization time distributions from the calculations where electron correlation is excluded during SDI (see text for details). (b)-(d) The ionization time distributions of the first electron versus the second electron for the SDI events in (a)-(c) respectively. The CEP of the pulses are set to be zero.

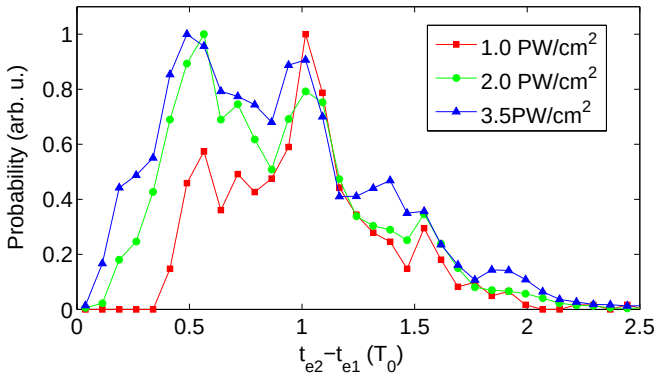

Fig. 4. The time delay between the ionization of the first and the second electrons. The laser parameters are the same as those in Fig. 3

the ionization in SDI. Very recently, with a semiclassical monte carlo method where the electron correlation is completely excluded, it has been demonstrated that the subcycle ionization bursts sensitively depend on the laser parameters, such as pulse envelope, duration, chirp, intensity [43]. Changing these laser parameters (the laser intensity in our case) will significantly affects the subcyle ionization bursts [43] and thus could result in the laser-parameter-dependent ratio of parallel and antiparallel emissions. It implies that the electron-correlations is not necessary for the experimentally observed oscillating behavior. Of course, one could expected that the electron correlation could also affect the subcyle ionization bursts [32]. The uncertainty of the parameters in experiment makes it impossible to have a quantitative comparison of the numeri-

Optics EXPRESS

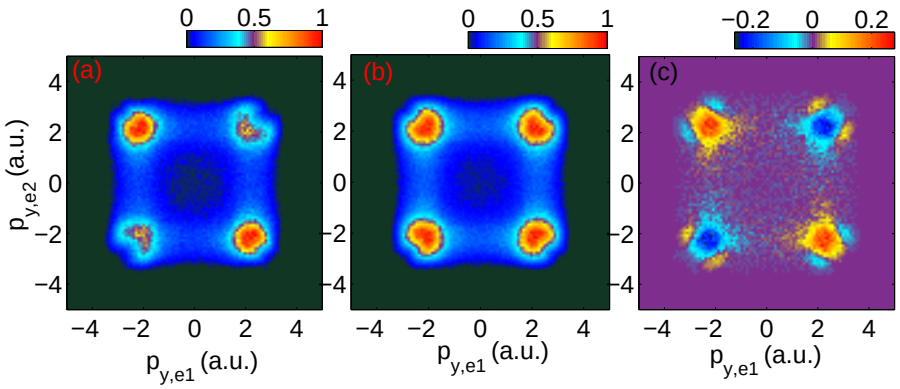

Fig. 5. (a) The differential electron momentum distribution. The $\hat{\mathbf{x}}$-axis and $\hat{\mathbf{y}}$-axis represent the momenta of the first and second electrons along the minor axis of the laser polarization plane. Here, the two electrons are not distinguished. (b) The differential momentum distribution for the "noncoincidence" data (see text for details) where the shapes of the distributions for the parallel and antiparallel emission SDI events are the same. (c) the difference between (a) and (b), obtained by subtracting (b) and the CEP is randomly set for each trajectory. The focal volume effect has been taken into account.

cal and experimental data. Thus, it is difficult to identify to what extent the oscillation is from the electron correlation and to what extent it is a consequence of the laser-parameter-dependent subcycle ionization dynamics. Nevertheless, in our classical simulations, we can check the role of electron correlation by artificially turned off the electron-electron interaction. This is done by permitting only one electron to be active during the ionization of Ar. After the first electron is ionized, the second electron is allowed to become active, and subject to removal from Ar^+. In this way the electron correlation is excluded during SDI. The ionization time distributions of the two electrons in these calculations are presented in Figs. 3(a)-3(c) (the yellow squares and green circles). It is shown that the distributions are almost the same as these from the calculations where the electron interaction is included. This indicates that in our classical model electron correlation plays a negligible role in the oscillating ratio of parallel and antiparallel emissions.

In the previous experiment [32], another evidence of electron correlation was expressed in the differential electron momentum distribution along the minor axis of the laser polarization plane. It was expected that the shape of the distribution should be the same for the parallel and antiparallel emission SDI events if the two electrons are independent. However, the experiment observed subtle difference in the shapes of the distributions for the parallel and antiparallel emissions [32]. In Fig. 5(a) we show the differential momentum distribution from our calculations. The distribution is symmetric about the diagonal because we did not distinguish the first and the second electrons here. The difference of the distributions for the parallel (the first and third quadrants) and antiparallel (the second and fourth quadrants) emissions is visible in our numerical results. To see this difference more clearly, we first generated a set of data by exchanging the distributions in the first (third) and second (fourth) quadrants, and then added this set of new data to Fig. 5(a), which yields the same shape of the distributions in the first (third) and second (fourth) quadrants, as shown in Fig. 5(b). The difference for the parallel and antiparallel emission events is now more clearly seen by subtracting Fig. 5(b) from Fig. 5(a), as shown in Fig. 5(c). This difference could also be explained within the independent electron approxima-

Optics EXPRESS

tion by considering the subcycle ionization bursts as demonstrated above. In the elliptical laser fields, electron's momentum is related to the ionization time. The momentum difference of the two electrons depends on the time delay between the ionizations. For the parallel and antiparallel emission SDI events, the ionization time delay and thus the difference in the two electrons' final momenta are different, resulting in the slightly different shapes in the differential electron momentum distributions, as displayed in Figs. 5(a) and 5(c).

4. Conclusion

In summary, we revisited the experimental features of electron correlation in SDI. We show that the experimentally observed oscillating behavior in the ratio of parallel and antiparallel emissions, and the difference in the shapes of the differential electron momentum distributions for the parallel and antiparallel emission SDI events, could be well explained as the subcycle ionization bursts in SDI. This subcycle ionization dynamics is very sensitive to the laser parameters [41, 43], . Moreover, our calculations based on the classical model shown that the electron correlation plays a negligible role in the subcycle ionization dynamics in SDI. Thus, the laser-parameter-dependent subcycle nature of the ionization dynamics alone can explain these features, without resorting to the arguments based on the electron-electron correlation. Therefore, these features are not enough to claim the breakdown of the independent electron approximation in SDI. Admittedly, the electron correlation can not be exclusively ruled out in SDI based on the existing experimental data. It requires more accurate experiments as well as more elaborate theoretical methods to identify how well the independent electron approximation works in SDI.

Funding

National Natural Science Foundation of China (NNSFC) (11622431, 61405064, 11234004, 11547018).

Acknowledgments

Numerical simulations presented in this paper were carried out using the High Performance Computing Center experimental testbed in SCTS/CGCL (see http://grid.hust.edu.cn/hpcc).